Oxidation of Phenol in Aqueous Acid: Characterization and Reactions of Radical Cations vis-à-vis the Phenoxyl Radical

Tomi Nath Das[†]

Radiation Chemistry & Chemical Dynamics Division, B.A.R.C., Trombay, Mumbai 400 085, India

Received: January 3, 2005; In Final Form: February 23, 2005

Aqueous sulfuric acid containing up to ~14 M acid ($H_0 \geq -7.0$) was used as solvent in pulse radiolytic redox studies to characterize cationic transients of phenol (C_6H_5OH) and map their reactions. The primary radical yields were first measured to correlate the variation in various radical concentrations as a function of increasing acid fraction in the solvent. Compared to their respective values at pH 2, the $G(Ox^{\bullet})$ increased with almost a linear slope of ~0.024 μmol J^{-1} for H_0^{-1} (or pH^{-1}) up to H_0 −6.0 ($Ox^{\bullet} = {}^{\bullet}OH + SO_4^{\bullet-}$), whereas $G(H^{\bullet})$ increased with a slope of ~0.033 μmol J^{-1} for H_0^{-1} (or pH^{-1}) up to H_0 −5.0. In the presence of >10 M acid ($H_0 < -5.0$), phenol was oxidized to its radical cation, $C_6H_5OH^{\bullet+}$, which further reacted with phenol and generated the secondary, dimeric radical cation, $(C_6H_5OH)_2^{\bullet+}$, following an equilibrium reaction $C_6H_5OH^{\bullet+} + C_6H_5OH \rightleftharpoons (C_6H_5OH)_2^{\bullet+}$, with $K_{eq} = 315 \pm 15\ M^{-1}$. The two cationic radicals were characterized from their individual UV−vis absorption spectra and acidity. The $C_6H_5OH^{\bullet+}$ absorption peaks are centered at 276 and 419 nm, and it was found to be more acidic ($pK_a = -2.75 \pm 0.05$) than $(C_6H_5OH)_2^{\bullet+}$ ($pK_a = -1.98 \pm 0.02$), having its major peak at 410 nm. On the other hand, in the presence of <6.5 M acid the $C_6H_5O^{\bullet}$ reactions followed the radical dimerization route, independent of the parent phenol concentration.

Introduction

Phenolic chemistry in a variety of application areas such as auto- and anti-oxidation, biochemical synthesis, the dye, pesticide and drug industry, stabilizers in polymers and plastics, atmospheric and water pollution control, etc. involving its oxidative reactions, or related reductive pathways of related quinonoidic compounds[1a−c] are generally discussed in terms of generation and reactions of the appropriate phenoxyl radical as the reactive intermediate.[1d,e] Even in the case of phenol (C_6H_5OH), which often serves as a convenient reference or model system for these phenolic compounds, the phenoxyl radical, $C_6H_5O^{\bullet}$ is considered to be the predominant *semi-oxidized* species, and hardly any information is available regarding the chemical behavior of its conjugate acid, the phenol radical cation, $C_6H_5OH^{\bullet+}$. In most oxidative reactions though (other than a direct H-abstraction), the formation of $C_6H_5O^{\bullet}$ would necessitate a favorable deprotonation of the intermediate $C_6H_5OH^{\bullet+}$, formed first in reaction 1.

$$C_6H_5OH - e^- \rightarrow C_6H_5OH^{\bullet+} (+H_2O) \rightleftharpoons C_6H_5O^{\bullet} + H_3O^+ \quad (1)$$

The lone measurement in aqueous acid medium reports that $C_6H_5OH^{\bullet+}$ deprotonation occurs at H_0 −4.8 (Hammett acidity function scale, the proton activity corrected pK_a being −2.0).[2] Thus, $C_6H_5OH^{\bullet+}$ possibly remained elusive in mildly acidic aqueous medium employed so far in other time-resolved phenol oxidation studies, although its presence otherwise has been reported in nonaqueous medium, in gas phase and in frozen matrix.[3−5]

A scrutiny of the experimental procedure of the previous study,[2] however, reveals that phenol oxidation in aqueous sulfuric acid medium was carried out with Ce(IV) under a steady-state condition. The ensuing semi-oxidized phenol radicals were supposedly detected by their time-averaged esr signal, but any likely interference from radical−radical, radical−solvent and radical−solute(s) type reaction product(s) was not checked. Thus, a confirmation of the real time radical stability therein was missing, although a time resolution of ≥100 μs was otherwise available then for transient detection by esr.[6] Recently, it has been shown by quantum chemical calculations that in the gas phase, as a result of favorable intermolecular hydrogen bonding (and also simultaneous aromatic−aromatic attraction), both phenol[7a−c,8a] and its cation[8b] add to another phenol molecule and produce the more stable, respective dimeric species. Additionally, it is reported that due to favorable hydrogen bonding, a number of water molecules can sequentially get attached to the radical cations forming different cationic clusters.[9a,b] In light of these theoretical revelations, doubts now arise about the assumed chemical stability of $C_6H_5OH^{\bullet+}$, and it seems plausible that the cation might not have been detected exclusively, or might have missed out completely in the presence of the prevailing ≥1 cM phenol concentration.[2] As a result, even the reported radical acidity value could have arisen due to another cationic species. A complete time-resolved reevaluation of phenol oxidation via the cationic route is therefore overdue, both for unequivocal $C_6H_5OH^{\bullet+}$ generation and for characterization, as well as for an update of its chemistry. Only then may the existing knowledge of phenol oxidation be complemented.

Taking a cue from the previous study,[2] the solution acidity in our measurements was set as before, following the Hammett acidity function scale[10] (H_0) but the real-time mapping of radical generation and decay was achieved with the pulse radiolytic (PR) oxidative route. In the present PR measurements, perchloric acid use was restricted mainly due to the attainable upper acidity limit of its solutions (H_0 −5.3).[10] Only H_2SO_4 allows measurements even at $H_0 < -5.3$ and the first part of our measurements

[†] E-mail: tndas@apsara.barc.ernet.in.

10.1021/jp050015p CCC: $30.25
Published on Web 03/25/2005

describes the specific details of such experimental protocols and quantification of various physical parameters essential for maintaining the desired oxidizing condition. In the second part, generation of semi-oxidized phenol species, their temporal behavior and reactions over a time scale of sub microseconds to seconds are presented. These measurements reveal the importance of secondary radical reactions and also provide the updated radical acidity values.

Experimental Section

Materials and Procedure. Water used in these studies was obtained from Millipore Gradiant A10 system, with conductivity >18 MΩ cm^{-1} and organic carbon <5 ppb. The gases O_2, Ar, N_2 and N_2O used for purging were obtained locally from British Oxygen Ltd. (purity ≈ 99.95%). $HClO_4$ solution (62 wt %) and H_2SO_4 (98 wt %) were obtained locally from SD Fine Chemicals and Thomas Baker, respectively, and used without further purification. Phenol used in this study was the best purity grade available from Lancaster. It is pertinent to note here that in high sulfuric acid concentrations (>14 M), irreversible sulfonation of phenol has been reported in a previous study.[11] Therefore the upper limit of solution acidity was restricted to ∼14 M whereas the corresponding solution H_0 values were set following the details available in the literature.[10] As a precautionary check on phenol stability, its absorption spectrum in appropriate O_2 saturated acid solutions was always verified prior to a PR study. These spectral measurements were made on a Hitachi 2001 spectrophotometer. In the concentration range of 4 μM to 5 cM, phenol remained (chemically) stable for at least 30 min after mixing in acid solution. In PR measurement, the phenol sample was always added to the acid medium immediately before pulsing and any possibility of its thermal decomposition was therefore ruled out. All measurements were carried out at ambient temperature close to 25 ± 1 °C.

The reported gas-phase stabilization energy of ∼6 kcal mol^{-1} for the $(C_6H_5OH)_2$ species[8b] led us to check its presence in the samples. Because the phenol spectral profile remained unchanged when its concentration was increased from 4 μM to 5 cM, it is assumed that in aqueous acid the $(C_6H_5OH)_2$ species is absent. Additionally, in the absence of a definite spectral support for the presence of the protonated species, $C_6H_5OH_2^+$ even at H_0 −7.0, phenol is uniformly represented as C_6H_5OH throughout this presentation.

The 7 MeV pulse radiolysis-kinetic spectrophotometric detection setup used in this study and the data analysis protocols have been described in detail before.[12,13] Briefly, samples were irradiated in a 1 cm × 1 cm square Suprasil cell. Optical detection of transients and related measurements was performed within the spectral range of 250−800 nm using a 450 W xenon lamp and a Kratos monochromator blazed at 300 nm coupled to a Hamamatsu R-955 photomultiplier tube. A spectral resolution of ≈1 nm could be achieved whereas the background signal at 250 nm due to scattered light remained <2%. Sample replenishment before each pulse was made with the help of a flow arrangement and oscilloscope traces were averaged during spectral and kinetic measurements. Polytetrafluoroethylene (PTFE) tubing was used for the entire flow system, with acid resistant Viton tubing used for pumping. A 1 cM aerated SCN^- solution was used for routine dosimetry, taking $G \times \epsilon = 2.59 \times 10^{-4}$ m^2 J^{-1} and $\epsilon = 7650$ M^{-1} cm^{-1} at 475 nm.[14] (The absorbed dose later in the text always refers to the equivalent dose measured as such.) The measured values from pulse radiolysis experiments generally have an uncertainty of ±10−15% and it applies to all subsequent results of this study.

Results and Discussion

Primary Radical Yields in Aqueous Acid. With an increase in acid fraction in the solvent, in addition to the $^{\bullet}OH$ and $H_2O_2^{\bullet+}$/$HO_2^{\bullet}$ radicals from reaction 2, other oxidizing radicals such as $SO_4^{\bullet-}$, $ClO_3^{\bullet}$ and $ClO_4^{\bullet}$ are generated following reactions 3 and 4.

$$H_2O \rightsquigarrow {}^{\bullet}OH,\ H_2O_2^{\bullet+}/HO_2^{\bullet},\ H^{\bullet},\ e_{aq}^{-},\ \text{etc.} \qquad (2)$$

$$^{\bullet}OH + H_2SO_4/HSO_4^{-} \rightarrow SO_4^{\bullet-} \quad \text{(and direct radiolysis of } H_2SO_4/HSO_4^{-}) \qquad (3)$$

$$HClO_4/ClO_4^{-} \rightsquigarrow ClO_3^{\bullet}\ \&\ ClO_4^{\bullet} \qquad (4)$$

In molar H_2SO_4 solution $SO_4^{\bullet-}$ forms both by the direct radiation chemical effects on H_2SO_4/HSO_4^- ($pK_{a1} = -10.0$, $pK_{a2} = 1.9$),[15] and also by the $^{\bullet}OH$ reactions ($k_{^{\bullet}OH+H_2SO_4} = 1.4 \times 10^7$ M^{-1} s^{-1} and $k_{^{\bullet}OH+HSO_4^-} = 4.7 \times 10^5$ M^{-1} s^{-1}).[16] In the case of $HClO_4$, $ClO_3^{\bullet}$ and $ClO_4^{\bullet}$ are formed only by the direct radiation chemical effects shown in reaction 4.[17] In reaction 2, the commonly denoted $HO_2^{\bullet}$ radical is presented in its protonated form on the basis of its reported pK_a value of 1.2 ± 0.3, equilibrium 5.[18]

$$H_2O_2^{\bullet+} + H_2O \rightleftharpoons HO_2^{\bullet} + H_3O^+ \qquad (5)$$

In acid solution, $H^{\bullet}$ (H-atom) becomes the primary reducing species as a result of "inside-spur protonation" of e_{aq}^- following reaction 6.

$$e_{aq}^{-} + H_3O^+ \rightarrow H^{\bullet} \qquad (6)$$

During oxidative measurements, $H^{\bullet}$ interference was best minimized by saturating the solutions with O_2; the reported k_7 value of 1.2×10^{10} M^{-1} s^{-1} at low pH[19] decreased steadily and reached a value of $\sim 7.0 \times 10^9$ M^{-1} s^{-1} at H_0 −7.[20]

$$H^{\bullet} + O_2\ (+H_3O^+) \rightarrow H_2O_2^{\bullet+} \qquad (7)$$

Although $HO_2^{\bullet}$ reaction with phenol is not yet reported, at the appropriate acidity, $H_2O_2^{\bullet+}$ may act as the oxidant. The thermodynamic support for such a reaction arises from the higher $H_2O_2^{\bullet+}$ reduction potential ($E^0 \sim 1.5$ V at pH 0)[21,22] as compared to phenol ($E^0 \sim 1.36$ V).[23] A check on such reaction kinetics was made by employing O_2 saturated pH 0 to H_0 −2.5 solutions containing 1 M H_2O_2. Then the after-pulse $H_2O_2^{\bullet+}$ yield was enhanced to the maximum value of ∼0.7 μM J^{-1}.[19,24,25] However, further addition of 200−500 μM phenol did not show the formation of $C_6H_5O^{\bullet}$; hence further involvement of $H_2O_2^{\bullet+}$ in our studies was ruled out.

Acid Dependent Yield of Primary Radicals. The dependency of primary oxidizing and reducing radical yields, $G(Ox^{\bullet})$ and $G(H^{\bullet})$ on the increasing acid concentration were separately measured and are consolidated in Figure 1. The $G(H^{\bullet})$ values were obtained by extending our recent measurements to higher acid concentrations.[20,26] Employing Ar saturated solutions (in the presence of 0.15 M *tert*-butyl alcohol) of either (i) ∼150 μM biphenyl or (ii) ∼250 μM I_2, the ensuing biphenyl H-adduct ($\epsilon_{360\ nm} = 5000$ M^{-1} cm^{-1})[27] or $I_2^{\bullet-}$ ($\epsilon_{380nm} = 9400$ M^{-1} cm^{-1})[28,29] concentrations were respectively estimated from the ΔA_{max} values assuming >95% conversion efficiency in each case. Any contribution from $SO_4^{\bullet-}$ absorption was separately estimated from its 470−500 nm kinetic traces and appropriately deducted.

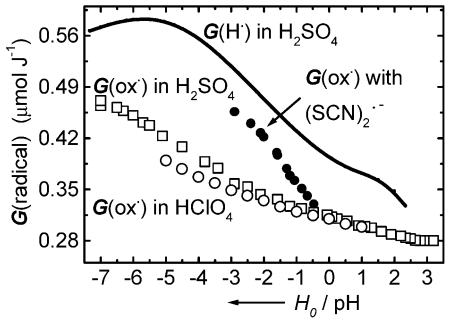

Figure 1. $G(Ox^{\bullet})$ and $G(H^{\bullet})$ in aqueous acid.

On the other hand, $G(Ox^{\bullet})$ estimation by routine thiocyanate dosimetry[14] was found to be unsuitable in molar acid solution. Deviations shown in Figure 1 were noticed possibly due to the HSCN deprotonation occurring at -1.1,[30] and partial $H^{\bullet}$ assisted oxidation of $HSCN/SCN^{-}$ (although such details are not yet known completely).[31] Additionally, in $HClO_4$ solution at $H_0 < -2.5$, HSCN was thermally oxidized. The correct $G(Ox^{\bullet})$ values were instead obtained from the following measurements.

Employing O_2 saturated 1 cM solution of the halide ion, X^{-} ($X^{-} = Cl^{-}$ or Br^{-}), $\sim$ 98% efficiency was achieved for $X_2^{\bullet-}$ generation following reactions 8 and 9.

$$X^{-} + Ox^{\bullet} \rightarrow X^{\bullet} \tag{8}$$

$$X^{\bullet} + X^{-} \rightarrow X_2^{\bullet-} \tag{9}$$

$Br_2^{\bullet-}$ concentration was measured at its λ_{max} 357 nm by taking $\epsilon_{357nm} = 9900\ M^{-1}\ cm^{-1}$,[32] whereas the $Cl_2^{\bullet-}$ concentration was measured at its λ_{max} 335 nm by taking $\epsilon_{335nm} = 8800\ M^{-1}\ cm^{-1}$.[33] These $X_2^{\bullet-}$ concentration estimates were suitably updated after accounting for minor radical loss within the time scale of respective measurements. The extent of each $X_2^{\bullet-}$ loss was judged separately from its own acid-dependent decay kinetics. HBr and HCl pK_a values being -9 and -8, respectively, these measurements could be satisfactorily performed over the entire acidity range, revealing the uniform set of $G(Ox^{\bullet})$ values. In presence of >3 M H_2SO_4, even $SO_4^{\bullet-}$ absorption (at λ_{max} 445 nm, taking $\epsilon_{445nm} = 1630\ M^{-1}\ cm^{-1}$)[13] could be directly used to measure the $G(Ox^{\bullet})$ value (once again taking into account any radical loss).

For these measurements, it was assumed that none of these radicals were protonated within the experimental acidity range, and consequently their respective ϵ value remained unchanged. This assumption was supported by the individual radical overlapping spectral profiles obtained at the highest solution acidity and at pH $\sim$ 0. Matching $G(Ox^{\bullet})$ values obtained with $Br_2^{\bullet-}$, $Cl_2^{\bullet-}$ and $SO_4^{\bullet-}$ support this assumption. Relative $G(Ox^{\bullet})$ values obtained in $HClO_4$ are marginally lower than the ones obtained in H_2SO_4 solutions, mainly due to the overall differences in the generation processes of the respective $Ox^{\bullet}$ in the two media. These measurements took care of the combined effects of the continuous change of radiation energy partition between the two solvent components,[34,35] and the subpicosecond trapping and scavenging of the quasi-dry electron by H_3O^{+} (resulting in a continuous increase in radical yields due to the reduced propensity of the "inside-spur" $H^{\bullet} + {}^{\bullet}OH$ reaction as compared to a faster $e_{aq}^{-} + {}^{\bullet}OH$ reaction occurring in solution of pH > 0[36]). In all subsequent measurements, the experimental $G(Ox^{\bullet})$ and $G(H^{\bullet})$ values from Figure 1 were used to normalize various transient yields at any chosen acidity.

Dissolved O_2 and $H^{\bullet}$ Interference. During oxidative studies in aqueous solutions, only dissolved O_2 was found suitable for scavenging $H^{\bullet}$. From our recent measurements,[20] using the acid dependent $[O_2]$ and $k_{H^{\bullet}+O_2}$ values, $H^{\bullet}$ scavenging potency of O_2 was quantified. The resulting plot is shown in Figure 2. All the currently relevant kinetic values and also the other ones discussed later were estimated to account for any effect of gradual change in H_2SO_4 solution viscosity.[37] Briefly, these measurements reveal that $k^0_{(H^{\bullet}+C_6H_5OH)} = 1.7 \times 10^9\ M^{-1}\ s^{-1}$ (superscript 0 refers to solution pH) and $k^0_{(H^{\bullet}+O_2)} = 1.2 \times 10^{10}\ M^{-1}\ s^{-1}$)[19] continuously decrease with increasing acid concentration, and the respective k^{-7} values (superscript -7 refers to solution H_0) are $\sim$70% and $\sim$61% of their k^0 estimates. More importantly, these numbers suggest that $H^{\bullet}$ scavenging by O_2 (saturation condition) to be effective (i.e., >95%), experimental $[C_6H_5OH]_{max}$ need to be $\leq$90 μM at H_0 -7.0, proportionately increasing to the level of $\sim$330 μM for pH $\geq$ 0. However, in our study, some measurements were also necessary with phenol concentrations exceeding 1 cM. As expected then, irrespective of the nature of the gas used for saturating these solutions (i.e., Ar/N_2 or O_2), considerable amounts of the phenol-H-adduct(s) were generated after pulse, and these interfered with the proposed oxidative measurements. To judge the extent of such interference and eliminate it, phenol-H-adduct spectral characteristics and their reaction kinetics were separately quantified. The spectral measurements in Ar saturated solutions in the presence of 0.15 M *tert*-butyl alcohol are reproduced in Figure 3.[20] The characteristic $HO-C_6H_6^{\bullet}$ absorption band is obtained at 330$-$335 nm at $H_0 > -3.0$, as reported in the past,[19,38] whereas the 360 nm band observed at $H_0 < -5.5$ is ascribed to the conjugate $H_2O-C_6H_6^{\bullet+}$ absorption. When the acid dependent $H_2O-C_6H_6^{\bullet+}$ ΔA_{360nm} values in the Figure 3 inset are

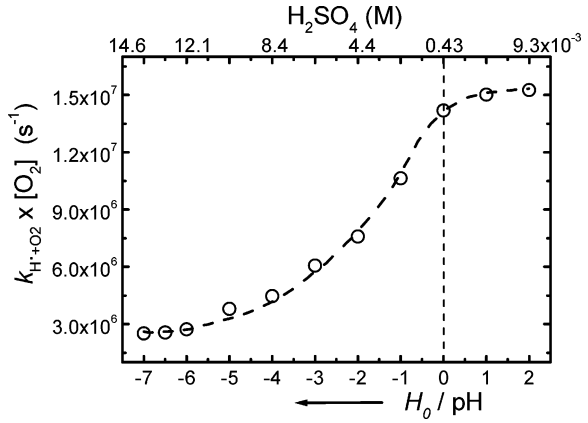

Figure 2. H-atom scavenging potency curve of O_2 in aqueous H_2SO_4 solution.

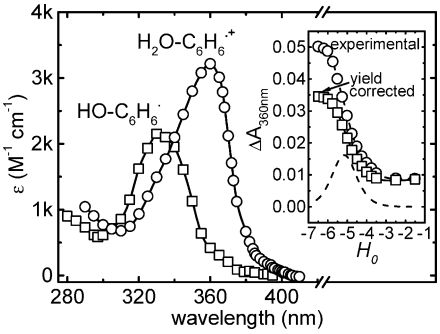

Figure 3. Phenol H-adduct absorption spectrum obtained with Ar saturated solution of 0.15 M *tert*-butyl alcohol and 300 μM phenol and irradiated with 10 Gy pulse ($SO_4^{\bullet-}$ contribution taken into account as explained in the text). (Inset) plot of ΔA_{360nm} against increase in acid concentration: experimental ΔA_{360nm} (○); yield corrected ΔA_{360nm} (□) and its relative first derivative (dashed line).

normalized with respect to the H$^\bullet$ yield (refer to Figure 1), the $[HO-C_6H_6^\bullet]/[H_2O-C_6H_6^{\bullet+}] = 1$ point is obtained at H_0 −5.3. Following the earlier methodology,[2] the proton activity corrected $H_2O-C_6H_6^{\bullet+}$ pK_a is obtained as −2.4. In these measurements, any interference due to $SO_4^{\bullet-}$ or the semi-oxidized phenol at the concerned wavelengths and time windows were separately estimated and suitably accounted.

In the case of other measurements when H$^\bullet$ scavenging by dissolved O_2 was not complete, then, in addition to the after-pulse interference due to $HO-C_6H_6^\bullet$ or $H_2O-C_6H_6^{\bullet+}$, at slower time scales, interference also appeared due subsequent peroxyl radical formation. Its magnitude was judged from radical formation/decay kinetics and spectral characteristics as follows. The rates of O_2 addition to $HO-C_6H_6^\bullet$ and $H_2O-C_6H_6^{\bullet+}$ were measured in solutions saturated with different ratios of N_2 and O_2. The measured k^0 value (=5.1×10^8 M^{-1} s^{-1}; its reported value being $(3.1-5.0) \times 10^8$ M^{-1} s^{-1})[39-41] decreased steadily with an increase in acid concentration and reached a k^{-7} value of 1.1×10^8 M^{-1} s^{-1}. The peroxyl radical spectral interference was considered on the basis of its reported absorption (ϵ_{310} = 690 M^{-1} cm^{-1}),[40] whereas its reported radical−radical decay rate ($k^{aq} = 4.7 \times 10^8$ M^{-1} s^{-1})[40] was assumed to have a $1/\eta$ dependency in the experimental medium.

Some of these spectral measurements were repeated in $HClO_4$ solutions mainly to analyze the extent of $SO_4^{\bullet-}$ interference encountered in H_2SO_4 solutions. Additionally, any occurrence of phenol-H-adduct + semi-oxidized phenol type inter-radical reaction was also checked. Covering a range of [*tert*-butyl alcohol]/[O_2] values, and also by changing the irradiation dose, the individual radical concentration as well as their concentration ratio was varied. However, the individual decay kinetics of either type of radical remained unaffected, suggesting a low propensity for inter-radical reactions.

Oxidation of Phenol in Low Acid Concentration. Although previous studies suggest use of $Cl_2^{\bullet-}$ as the oxidant for $C_6H_5O^\bullet$ generation in acidic pH,[42-44] the reported rate constant of phenol + $Cl_2^{\bullet-}$ reaction ($k^{1-2.5} = (2.5-5) \times 10^8$ M^{-1} s^{-1})[42-44] stipulates use of at least millimolar phenol and decimolar Cl^- concentrations. Only then can the direct $^\bullet$OH addition generating the OH-substituted hydroxycyclohexadienyl type radical ($HO-C_6H_5^\bullet OH$) be minimized.[38,45,46] Although the latter is also transformed into $C_6H_5O^\bullet$ under conducive solution acidity,[39,47,48] keeping in perspective the complex set of reactions leading to $Cl_2^{\bullet-}$ generation from the $^\bullet$OH + Cl^- reaction,[13] and the unavoidable generation of some phenol-H adduct in the presence of millimolar phenol, the feasibility of $C_6H_5O^\bullet$ generation without the use of Cl^- was checked. Transient spectral measurements made with $^\bullet$OH (as Ox$^\bullet$ in reaction 10) are shown in Figure 4.

$$C_6H_5OH + Ox^\bullet \rightarrow [C_6H_5OH]_{Ox} \qquad (10)$$

In this case, the difference in the transient spectral profiles obtained at H_0 −1.6 (similar to pH 12 results obtained with $N_3^\bullet$) and pH 2.2 shows only the presence of $HO-C_6H_5^\bullet OH$ with its characteristic absorption at 295−340 nm. With an aim to reduce the after-pulse $HO-C_6H_5^\bullet OH$ generation, as the solution pH was gradually reduced from 3 to 0 under O_2 saturation, Henderson−Hasselbalch type plots were obtained for G(Ox$^\bullet$) normalized $C_6H_5O^\bullet$ ΔA_{max} values obtained at 288/383/400 nm. Some of these plots are shown in the Figure 5 inset. The corresponding midpoint values (maximum slope) are obtained as 0.71 (at 288 nm, not shown), 0.69 (400 nm) and 0.72 (383 nm). When these measurements were repeated under N_2 saturation (then also taking into account contribution from the

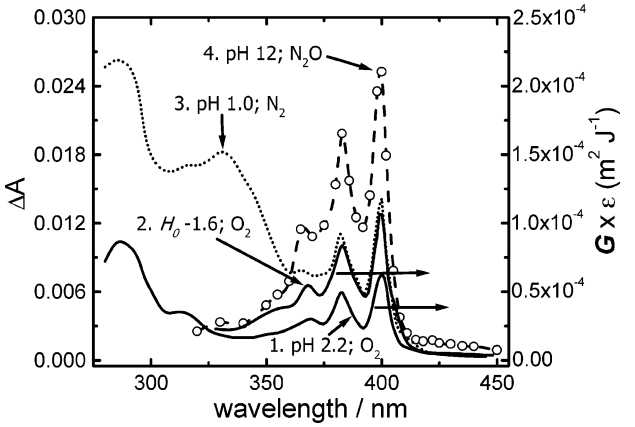

Figure 4. Transient (mostly $C_6H_5O^\bullet$) spectrum at different acidities (or alkalinities): (1) and (2) obtained with O_2 saturated 300 μM phenol solution and irradiated with 12.5 Gy pulse; (3) obtained with N_2 saturated 1 cM phenol solution (12.5 Gy); (4) obtained with N_2O saturated 1 cM N_3^- and 500 μM phenol solution (12 Gy).

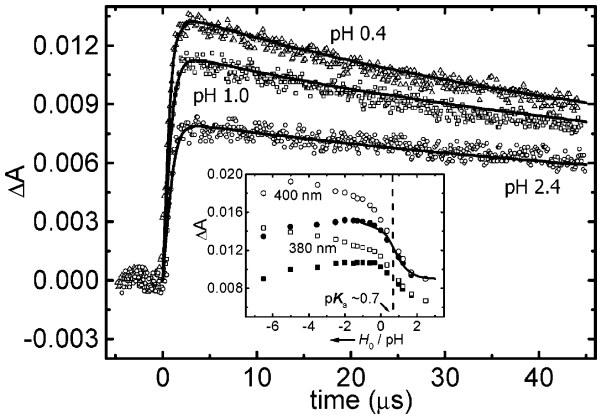

Figure 5. ACUCHEM overlay of 400 nm $C_6H_5O^\bullet$ formation/decay traces obtained at different pHs with O_2 saturated 240 μM phenol solution and irradiated with a 15 Gy pulse. (Inset) change in $C_6H_5O^\bullet$ yield with pH/H_0. The deprotonation type plot (maximum slope at pH ~ 0.7) is explained with the set reactions in Appendix A. (Inset) experimental values (open symbols); G(Ox$^\bullet$) yield corrected values (solid symbols). The solid line overlaying the 400 nm yield corrected values is obtained from ACUCHEM analysis of respective kinetic traces.

H-atom reaction), the S-type curves were replaced with plots showing a gradual increase in $C_6H_5O^\bullet$ yield with a decrease in solution pH. In this case the corresponding $C_6H_5O^\bullet$ yield was also found to be higher than the values obtained under O_2 saturation. The unchanged $C_6H_5O^\bullet$ spectral profile obtained in all these cases therefore suggests that the pK_a type value of 0.71 (averaged) arises as a result of $C_6H_5O^\bullet$ generation following more than one channel, depending both on solution acidity and on the presence of O_2.

In a recent study, similar dependency of $C_6H_5O^\bullet$ yield on acid concentration has been proposed, but the results therein were based on measurements made at pH > 3.[47] Satisfactory kinetic overlay of our pH 0−3 experimental traces was possible only after some of these projected rate values were updated by taking into account the prevailing acid concentration. The ACUCHEM multiparameter kinetic analysis software[49] was put to use and the reaction scheme shown in Appendix A was followed.

In this reaction set, the primary radical reactions *a*−*i* lead to $HO-C_6H_5^\bullet OH$ formation and $C_6H_5O^\bullet$ is subsequently generated from it following two reactions, *j* and *k*. Reaction *j* deals with the unimolecular water elimination whereas reaction *k* is acid

catalyzed. Reactions *l*, *m* and *n* deal with different HO−C_6H_5•OH loss processes.[47] Reactions *o* and *p* are necessary to include a partial $C_6H_5O^•$ decay even within the fast time scale of measurement. For data analysis it has been assumed that only $C_6H_5O^•$ absorbs at the wavelength of measurement (400 nm) and the hydronium ion is represented as H_3O^+. Our results suggest that although the published rate values of reactions *l*, *m* and *n* are adequate,[47] the rate values for reactions *j* and *k* shown within parentheses are unsuitable as these produced large differences in kinetic fitting. Although all these rate values (reactions *j*−*n*) were earlier obtained from measurements made in solutions of pH ≥ 3, under the present conditions of actual higher acidity, suitable modification was found necessary only for the reaction *k* as it alone relates to the H_3O^+ concentration. Simultaneous modification of rate of reaction *j* was mandatory as only a unique combination of these two reactions rate values allowed the desired ACUCHEM fitting of the 400 nm kinetic traces at various pH, shown in Figure 5. Reactions *l*, *m* and *n* did not have any dependency on the actual solution acidity, and as expected, did not need any modification in their respective rate values. The quality of our kinetic overlays highlights the necessity of such pH dependent measurements. If these detailed kinetic analyses were overlooked, then merely from the estimate of transient ΔA_{max}, divergent and therefore erroneous ϵ value emerges. For example, an earlier report of the $C_6H_5O^•$ ϵ_{400nm} value (=2150 M^{-1} cm^{-1})[38] correlates with the pH 2.2 measurement, whereas another ∼25% higher value (=2625 M^{-1} cm^{-1})[51] suggests a slightly lower solution pH. On the other hand, our analysis reveals the correct pH independent $C_6H_5O^•$ ϵ_{400nm} value (=3550 ± 250 M^{-1} cm^{-1}). As a further support, an ϵ_{400nm} value = 3540 ± 200 M^{-1} cm^{-1} was also measured from an independent phenol oxidation measurement shown in Figure 4 in N_2O saturated pH 12 solution with $N_3^•$ as the oxidizing radical, taking the $G(N_3^•) = 0.6$ μmol J^{-1} following previous measurements.[52,53] The updated $C_6H_5O^•$ absorption spectrum (molar absorptivity vs wavelength) was used for obtaining the desired $C_6H_5OH^{•+}$ spectrum presented below.

Under O_2 saturation, when phenol concentration was appropriately maintained at ≤250 μM, only the three characteristic absorption peaks at 288/383/400 nm were observed up to H_0 −3.0, suggesting only $C_6H_5O^•$ generation. Employing $HClO_4$ solutions, the above results could be reproduced from pH 3 to H_0 −3.0.

Oxidation of Phenol at High Acid Concentration. Below H_0 −3.0, first a hump appeared around 410−425 nm in the after-pulse transient absorption profile, and with a further increase in acid concentration, new transient absorption peaks at 360−365 and 414 nm gradually emerged and gained in intensity. Concurrently, the intensity of the $C_6H_5O^•$ peaks at 383/400 nm gradually decreased, whereas its 288 nm peak shifted to higher energy. In N_2 saturated H_0 −7.0 solution of 1.5 mM phenol, the transient absorption spectrum (open symbol) shown in Figure 6 was recorded at 10 μs after end of pulse. Analysis of related kinetic traces recorded at various wavelengths suggested the presence of $H_2O-C_6H_6^{•+}$, $C_6H_5O^•$ and $SO_4^{•-}$ at this chosen time of measurement. To find their individual contributions in the transient spectrum, the relevant rate constants were measured separately at H_0 −7.0. These rate values are $k^{-7}_{(H_2O-C_6H_6^{•+}+H_2O-C_6H_6^{•+})} = 3.0 \times 10^8$ M^{-1} s^{-1} taken from our recent measurement,[20] $k^{-7}_{(^•OH+HSO_4^-)} = 1.0 \times 10^7$ M^{-1} s^{-1}, $k^{-7}_{(SO_4^{•-}+SO_4^{•-})} = 4.5 \times 10^8$ M^{-1} s^{-1}, $k^{-7}_{(SO_4^{•-}+C_6H_5OH)} = 2.1 \times 10^8$ M^{-1} s^{-1} (following 445 nm $SO_4^{•-}$ decay; for comparison, $k^{-1}_{(SO_4^{•-}+C_6H_5OH)} = 1.0 \times 10^9$ M^{-1} s^{-1}), and $k^{-7}_{(^•OH+C_6H_5OH)} = 7.2 \times 10^8$ M^{-1} s^{-1} (obtained from 277 nm transient formation after accounting for the slower contribution from above $k^{-7}_{(SO_4^{•-}+C_6H_5OH)}$). These kinetic measurements also revealed minor radical loss taking place at the selected time of measurement.

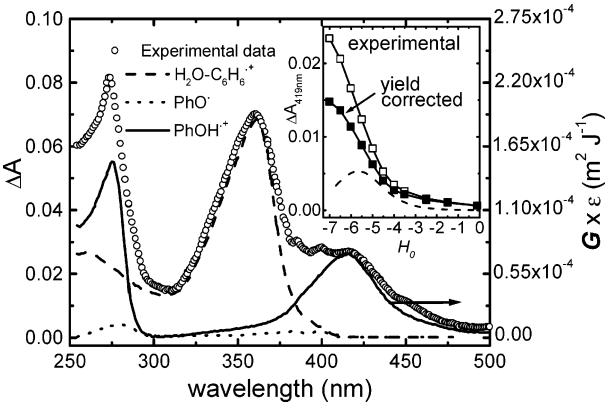

Figure 6. Transient absorption spectra in a N_2 saturated, H_0 −7.0 solution of 1.5 mM phenol irradiated with 36 Gy pulse, with contributions from various radicals explained in the text. (Inset) increase in $C_6H_5OH^{•+}$ absorption, ΔA_{419nm} with acid concentration: experimental ΔA_{419nm} (□); yield corrected ΔA_{419nm} (■) and its relative first derivative (dashed line).

Taking into account the absorbed dose, the $G(H^•)^{-7}$ (superscript −7 refers to solution H_0) value of 0.57 μmol J^{-1} from Figure 1, and the $H_2O-C_6H_6^{•+}$ spectral characteristics (from Figure 3, assuming its complete generation), its estimated spectral contribution is shown in Figure 6 (dashed line). On the other hand, from the absorbed dose and the $G(Ox^•)^{-7}$ value of 0.47 μmol J^{-1} from Figure 1, the $[Ox^•]_{max}$ was obtained. Because the kinetic analysis above revealed ∼10% not-yet reacted $SO_4^{•-}$ at the chosen 10 μs time window, the semi-oxidized phenol concentration was ∼90% of $[Ox^•]_{max}$. In the latter, ∼5% $C_6H_5O^•$ contribution (seen as 383/400 nm humps) was estimated from the plot of $G(Ox^•)$ yield corrected ΔA_{419nm} vs H_0 (Figure 6 inset). The updated $C_6H_5O^•$ absorption spectrum from the previous section was used to estimate its present contribution (dotted line). On subtraction of the $H_2O-C_6H_6^{•+}$, $C_6H_5O^•$ and $SO_4^{•-}$ absorptions, the difference spectrum in Figure 6 (solid line) shows two peaks at 277 nm (fwhm = 12 nm not considering C_6H_5OH bleaching correction) and 419 nm (fwhm = 50 nm). These are assigned to $C_6H_5OH^{•+}$ absorption, and from its calculated concentration (∼85% of $[Ox^•]_{max}$), the ϵ_{277nm} and ϵ_{419nm} values are respectively estimated as 3710 ± 250 and 1800 ± 150 M^{-1} cm^{-1}.

The $C_6H_5OH^{•+}$ λ_{max} values are reported at 275.5 and 423 nm in solid argon,[5] and 430−440 nm in organic solvents.[3b] On the other hand, the corresponding $C_6H_5O^•$ λ_{max} is always reported at 400 nm,[3b,4,5] as observed in aqueous medium. The blue-shift of the lower energy $C_6H_5OH^{•+}$ peak in aqueous acid possibly indicates a favorable solvent effect, thereby suggesting different origins of its two peaks. More importantly, further analysis of the Figure 6 inset plot reveals its maximum slope at H_0 −5.7 corresponding to the deprotonation reaction $C_6H_5OH^{•+} + H_2O \rightleftharpoons C_6H_5O^• + H_3O^+$. Following the methodology described in the previous study,[2] the proton activity corrected $C_6H_5OH^{•+}$ pK_a is calculated as −2.75 ± 0.05. The current solution acidity value of −5.7 for $C_6H_5OH^{•+}$ deprotonation is considerably different from the earlier report of −4.8.[2] A satisfactory answer for this discrepancy was obtained from the following measurements at time scale of >100 μs.

Slow Time-Scale Measurement at High Acid Concentration. Although in acid concentration <6.5 M, the $C_6H_5O^•$ decay

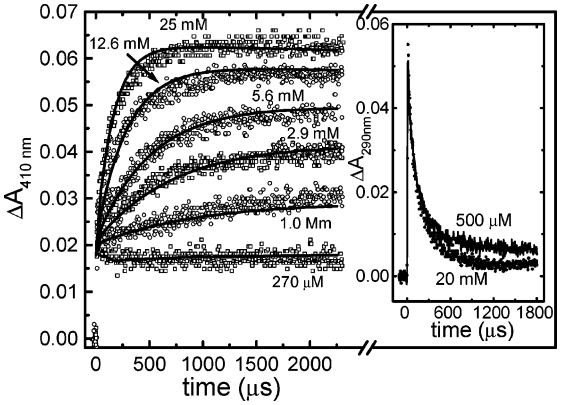

Figure 7. Transient formation kinetics at 410 nm in O_2 saturated, H_0 −7.0 solution of phenol irradiated with 29 Gy pulse. First order formation rate values 6.4×10^3; 3.5×10^3; 1.9×10^3; 1.6×10^3 and 1.1×10^3 s^{-1} are respectively obtained with 25 mM; 12.6 mM; 5.6 mM; 2.9 mM and 1 mM phenol concentration. (Inset) 290 nm $C_6H_5O^{\bullet}$ decay traces at H_0 −2.0 under O_2 saturation indicate the kinetics to be independent of phenol concentration.

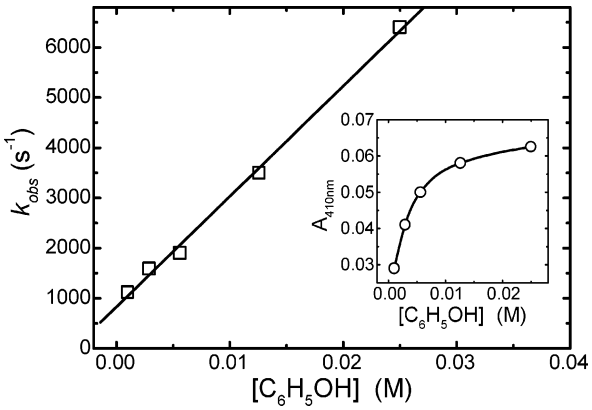

Figure 8. Variation of (first order) transient formation rates under experimental conditions described in Figure 7. (Inset) variation of observed secondary transient yield under the same experimental conditions.

remained independent of phenol concentration as postulated before[54] (Figure 7 inset), the nature of $C_6H_5OH^{\bullet+}$ decay in higher acid concentration was found to be of opposite nature. For example, H_0 −7.0 kinetic traces shown in Figure 7 reveal that as phenol concentration was increased from 270 μM to a few centimolar, a secondary transient ΔA as well as its formation rate, k_{obs}, were increased continuously, implying $C_6H_5OH^{\bullet+}$ reaction with the parent. However, as shown in Figure 8, the resulting plots of such changes in (i) k_{obs} and (ii) ΔA values against the prevailing phenol concentration are of dissimilar nature. While the rate of increase in k_{obs} values remained constant, the corresponding rate of increase in ΔA values gradually leveled off, thereby suggesting the proposed reaction 11 to be reversible.

$$C_6H_5OH^{\bullet+} + C_6H_5OH \rightleftharpoons (C_6H_5OH)_2^{\bullet+} \qquad (11)$$

The set for reactions shown in Appendix B was judged to the most appropriate one for ACUCHEM analyses of the formation traces shown in Figure 7. The desired rate values for this purpose were obtained as follows. Although the equilibrium 11 forward k_{11} (or $k_r = 2.2 \times 10^5$ M^{-1} s^{-1}) and reverse k_{-11} (or $k_s = 7.0 \times 10^2$ s^{-1}) values were obtained from analysis of Figure 8 data, the second-order decay rate of $C_6H_5OH^{\bullet+}$, k_t, was measured separately at 280 nm in a H_0 −7.0 solution of <50

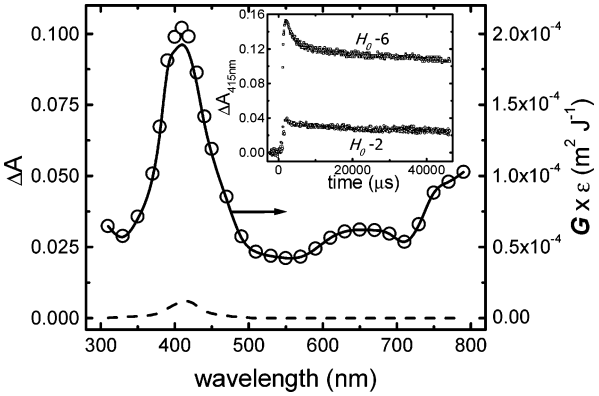

Figure 9. Secondary transient spectrum (○) obtained at 2 ms after pulse in O_2 saturated H_0 −7.0 solution of 1.5 cM phenol irradiated with 42 Gy pulse. Subtraction of $C_6H_5OH^{\bullet+}$ contribution (− − −) reveals the $(C_6H_5OH)_2^{\bullet+}$ absorption (—) (Inset) transient decay profiles obtained at H_0 −2.0 and −7.0 in the presence of 2.0 cM phenol.

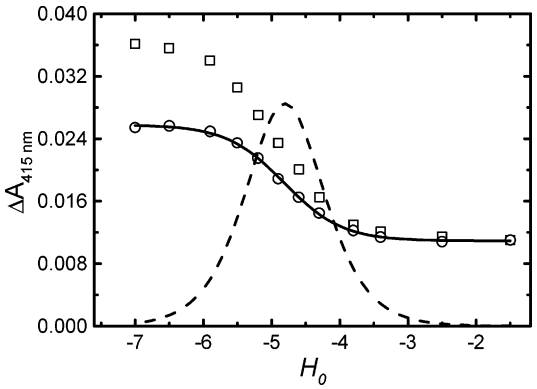

Figure 10. Transient absorbance obtained at 2.5 ms after pulse in O_2 saturated solution of 1 cM phenol solution irradiated with 20 Gy pulse: experimental ΔA_{max} (□); yield corrected ΔA_{max} (○), and its relative first derivative (dashed line).

μM phenol. The $(C_6H_5OH)_2^{\bullet+}$ decay rates k_u and k_v were estimated separately from further analysis of kinetic traces obtained in milliseconds to seconds time scale (a sample trace is shown in the Figure 9 inset). On the other hand, the proposed $(C_6H_5OH)_2^{\bullet+}$ absorption characteristics was obtained from the Figure 9 transient spectrum, recorded with a O_2 saturated H_0 −7.0 solution of 1.5 cM phenol. It was estimated that at the selected 2 ms time of measurement, 17.4% $C_6H_5OH^{\bullet+}$ contribution prevailed. After subtracting its contributions in the transient absorption, and taking >98% phenol oxidation efficiency, we estimated the $(C_6H_5OH)_2^{\bullet+}$ absorption spectrum and its desired ϵ_{410} value (5000 ± 500 M^{-1} cm^{-1}). Although further studies are underway to quantify the proposed tertiary radical $(C_6H_5OH)_3^{\bullet+}$ chemistry, the current contribution from its ϵ_{410nm} value of 9000 ± 1000 M^{-1} cm^{-1} was ∼0.2%.

As a result of the above exercise, a large variance in the respective reactivity of $C_6H_5OH^{\bullet+}$ and $(C_6H_5OH)_2^{\bullet+}$ in the presence of a few centimolar phenol is revealed. The concentration ratio $[(C_6H_5OH)_2^{\bullet+}]/[C_6H_5OH^{\bullet+}]$ then remains close to 6:1. Therefore, it is inferred that in the earlier steady-state measurement employing 2 cM phenol,[2] due to ready formation but a longer lifetime of $(C_6H_5OH)_2^{\bullet+}$ as compared to $C_6H_5OH^{\bullet+}$, the former had definitely interfered in the measurements aimed to detect the latter, possibly due to their structural similarity as revealed recently.[8a] As the previously reported $C_6H_5OH^{\bullet+}$ pK_a of −2.0[2] has already been proved to be incorrect, a supportive explanation regarding the nature of the reported radical deprotonation at H_0 −4.7[2] is also necessary. To check if $(C_6H_5OH)_2^{\bullet+}$

SCHEME 1

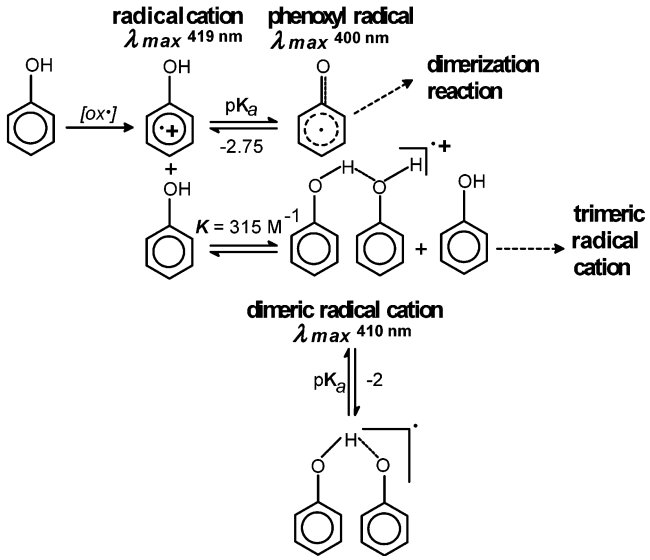

was the likely answer, its acid dependent yield was measured in the presence of 1 cM phenol. In Figure 10, a plot of 2.5 ms after-pulse ΔA_{415nm} values reveals a continuously increasing trend with increase in acid concentration. On normalization of the ΔA_{415nm} values, an S-type curve emerges and the resulting maximum slope at H_0 −4.8 is proposed to describe $(C_6H_5OH)_2^{\bullet+}$ deprotonation (due to its majority contribution at 2.5 ms), thereby confirming the above assumption. The proton activity corrected $(C_6H_5OH)_2^{\bullet+}$ pK_a value is estimated to be −1.98 ± 0.02.

Conclusions. In light of these results, the reactions in Scheme 1 emerge as the representative of free radical induced phenol oxidation in aqueous acid wherein the major difference lies in the preferred reactions of the cationic intermediate(s) with the parent, which is totally absent in case of $C_6H_5O^{\bullet}$ reaction. When these studies were repeated with $HClO_4$ (but restricted within the upper solution acidity limit of −5.3), reproducible results confirmed that the nature of the acid used had no influence either on the respective radical generation process or its subsequent chemistry. As a corollary it is proposed that the nature of acid would not have any role even at $H_0 < -5.3$. Current success with the use of aqueous H_2SO_4 solvent for pulse radiolytic redox reactions suggests that an entirely new methodology is now available for probing yet unknown free radical reactions, which can complement similar studies in nonaqueous solvents. Detailed quantum chemical calculations taking into account appropriate solvent effects may explain if the near-IR absorption band observed for $(C_6H_5OH)_2^{\bullet+}$ arises as a result of a charge resonance band postulated to appear in a sandwiched structure.[55,56]

Acknowledgment. I thank my colleagues Mr. Vijendra N. Rao, Drs. G. Bhaskar Dutt, Tushar Bandyopadhyay and Tulsi Mukherjee (Associate Director, Chemical Group) for their support during this study. I also thank Dr. Pedatsur Neta for previewing the revised manuscript and offering his valuable suggestions, and the reviewers of this manuscript for comments, suggestions and critical opinion on all aspects of the study.

Appendix A: Formation and Decay of $C_6H_5O^{\bullet}$ in O_2 Saturated Solution at Different pHs

Reactions and Rate Constants.

(*a*) $H^{\bullet} + {}^{\bullet}OH \rightarrow H_2O \qquad k = 7.0 \times 10^9\ M^{-1}\,s^{-1}$ [50]

(*b*) ${}^{\bullet}OH + e_{aq}^{-} \rightarrow OH^{-} \qquad k = 5.0 \times 10^{10}\ M^{-1}\,s^{-1}$ [50]

(*c*) ${}^{\bullet}OH + {}^{\bullet}OH \rightarrow H_2O_2 \qquad k = 5.5 \times 10^9\ M^{-1}\,s^{-1}$ [50]

(*d*) $H^{\bullet} + H^{\bullet} \rightarrow H_2 \qquad k = 5.0 \times 10^9\ M^{-1}\,s^{-1}$ [50]

(*e*) $e_{aq}^{-} + H_3O^{+} \rightarrow H^{\bullet} \qquad k = 2.3 \times 10^{10}\ M^{-1}\,s^{-1}$ [50]

(*f*) $e_{aq}^{-} + O_2 \rightarrow HO_2^{\bullet}/H_2O_2^{\bullet+} \qquad k = 1.9 \times 10^{10}\ M^{-1}\,s^{-1}$ [50]

(*g*) $H^{\bullet} + O_2 \rightarrow HO_2^{\bullet}/H_2O_2^{\bullet+} \qquad k = 2.0 \times 10^{10}\ M^{-1}\,s^{-1}$ [50]

(*h*) $H^{\bullet} + C_6H_5OH \rightarrow HO{-}C_6H_6^{\bullet} \qquad k = 1.7 \times 10^9\ M^{-1}\,s^{-1}$ [50]

(*i*) ${}^{\bullet}OH + C_6H_5OH \rightarrow HO{-}C_6H_5{}^{\bullet}OH \qquad k = 6.6 \times 10^9\ M^{-1}\,s^{-1}$ [50]

(*j*) $HO{-}C_6H_5{}^{\bullet}OH \rightarrow C_6H_5O^{\bullet} + H_2O$
$k = 2.0 \times 10^6\ s^{-1}$ (for -*p*- adduct $k = 1.8 \times 10^3\ s^{-1}$)[47]

(*k*) $HO{-}C_6H_5{}^{\bullet}OH + H_3O^{+} \rightarrow C_6H_5O^{\bullet} + H_2O + H_3O^{+}$
$k = 2.0 \times 10^7\ M^{-1}\,s^{-1}$
(for -*o*- & -*p*- *adduct* $k_{av} = 6.7 \times 10^8\ M^{-1}\,s^{-1}$)[47]

(*l*) $HO{-}C_6H_5{}^{\bullet}OH + O_2 \rightarrow (HO)_2C_6H_5O_2^{\bullet}$
$k = 1.2 \times 10^9\ M^{-1}\,s^{-1}$ [47]

(*m*) $(HO)_2C_6H_5O_2^{\bullet} + H_3O^{+} \rightarrow HO_2^{\bullet}/H_2O_2^{\bullet+} + HOC_6H_4OH$
$k = 1.3 \times 10^5\ M^{-1}\,s^{-1}$ [47]

(*n*) $HO{-}C_6H_5{}^{\bullet}OH + HO{-}C_6H_5{}^{\bullet}OH \rightarrow (HO{-}C_6H_5OH)_2$
$k = 1.0 \times 10^8\ M^{-1}\,s^{-1}$ [47]

(*o*) $C_6H_5O^{\bullet} + C_6H_5O^{\bullet} \rightarrow (C_6H_5O)_2$
$k = 2.0 \times 10^9\ M^{-1}\,s^{-1}$ (*this study*)

(*p*) $(C_6H_5O)_2 + C_6H_5O^{\bullet} \rightarrow HOC_6H_4C_6H_4O^{\bullet} + C_6H_5OH$
$k = 5.5 \times 10^9\ M^{-1}\,s^{-1}$ (*this study*)

Starting solute and after-pulse radical concentrations for the dose employed:

$[O_2] = 1.2 \times 10^{-3}$ M; $[C_6H_5OH] = 2.4 \times 10^{-4}$ M;
$[H_3O^{+}] = 0.6{-}1.0 \times 10^{-3}$ M; $[H^{\bullet}] = 9.0 \times 10^{-7}$ M;
$[{}^{\bullet}OH] = 4.3 \times 10^{-6}$ M; $[e_{aq}^{-}] = 4.1 \times 10^{-6}$ M

Appendix B: Effect of Phenol Concentration on the Equilibrium Yield of $(C_6H_5OH)_2^{\bullet+}$ in H_0 −7.0 Solution

Reactions and Rate Constants.

(*q*) $SO_4^{\bullet-} + C_6H_5OH \rightarrow C_6H_5OH^{\bullet+} \qquad k = 2.1 \times 10^8\ M^{-1}\,s^{-1}$

(*r*) $C_6H_5OH + C_6H_5OH^{\bullet+} \rightarrow (C_6H_5OH)_2^{\bullet+} \qquad k = 2.2 \times 10^5\ M^{-1}\,s^{-1}$

$$(s)\ (C_6H_5OH)_2^{\bullet+} \rightarrow C_6H_5OH^{\bullet+} + C_6H_5OH \qquad k = 7.0 \times 10^2\ s^{-1}$$

$$(t)\ C_6H_5OH^{\bullet+} + C_6H_5OH^{\bullet+} \rightarrow \text{Product1} \qquad k = 1.0 \times 10^6\ M^{-1}\ s^{-1}$$

$$(u)\ (C_6H_5OH)_2^{\bullet+} + C_6H_5OH \rightarrow (C_6H_5OH)_3^{\bullet+} \qquad k = 1.0 \times 10^2\ M^{-1}\ s^{-1}$$

$$(v)\ (C_6H_5OH)_2^{\bullet+} + (C_6H_5OH)_2^{\bullet+} \rightarrow \text{Product2} \qquad k = 1.0 \times 10^4\ M^{-1}\ s^{-1}$$

Starting solute and radical concentration:

$$[SO_4^{\bullet-}] = 1.37 \times 10^{-5}\ M;$$

$$[C_6H_5OH] = 2.7 \times 10^{-4} \text{ to } 2.5 \times 10^{-2}\ M$$

References and Notes

(1) (a) Yamaguchi M. *Synthetic uses of phenols*; Chapter 10. (b) Glezer V. *Environmental effects of substituted phenols*; Chapter 18. (c) Solomon, D. H.; Qiao G. G.; Caulfield M. J. *Polymers based on phenols*; Chapter 20. (d) Neta P.; Steenken S. *Radiation Chemistry of Phenols*; Chapter 15. (e) Steenken S.; Neta P. Transient Phenoxyl s: Formation and Properties in aqueous Solutions. In *The Chemistry of Phenols*; Rappoport, Z., Ed.; John Wiley & Sons, Ltd.: New York, 2003; Chapter 16.

(2) Dixon, W. T.; Murphy, D. *J. Chem. Soc., Faraday Trans. 2* **1976**, *72*, 1221.

(3) (a) Brede O.; Naumov S.; Hermann R. *Rad. Phys. Chem.* **2003**, *67*, 225 and references therein. (b) Ganapathi, M. R.; Hermann, R.; Naumov, S.; Brede, O. *Phys. Chem. Chem. Phys*. **2000**, *2*, 4947.

(4) Le, H. T.; Flammang, R.; Gerbaux, P.; Bouchoux, G.; Nguyen, M. T. *J. Phys. Chem. A* **2001**, *105*, 11582.

(5) Kesper, K.; Diehl, F.; Simon, J. G. G.; Specht, H.; Schweig, A. *Chem. Phys.* **1991**, *153*, 511.

(6) Hayon, E.; Simic, M. *Acc. Chem. Res.* **1974**, *7*, 114.

(7) (a) Connell, L. L.; Ohline, S. M.; Joireman, P. W.; Corcoran, T. C.; Felkera, P. M. *J. Chem. Phys.* **1991**, *96*, 2585. (b) Dopfer O.; Lembach, G.; Wright, T. G.; Müller-Dethlefs K. *J. Chem. Phys.* **1992**, *98*, 1933. (c) Hay, B. P.; Dixon, D. A.; Vargas, R.; Garza, J.; Raymond, K. N. *Inorg. Chem.* **2001**, *40*, 3922.

(8) (a) Ghosh, T. K.; Miyoshi, E. *Theor. Chem. Acc.* **2000**, *105*, 31. (b) Pejov L. *Chem. Phys. Lett.* **2003**, *376*, 11.

(9) (a) Hobza, P.; Burcl, R.; Spirko, V.; Dopfer, O.; Müller-Dethlefs, K.; Schlag, E. W. *J. Chem. Phys.* **1994**, *101*, 990. (b) Watanabe, H.; Iwata, S. *J. Chem. Phys.* **1996**, *105*, 420.

(10) Rochester, C. H. *Organic Chemistry. Acidity Functions*; Academic Press: London, 1970; Vol. 17. Jorgenson, M. J.; Hartter, D. R. *J. Am. Chem. Soc.* **1963**, *85*, 878. Yates, K.; Wai, H. *J. Am. Chem. Soc*. **1964**, *86*, 5408. Ryabova, R. S.; Medvetskaya, I. M.; Vinnik, M. I. *Russ. J. Phys. Chem*. **1966**, *40*, 182. Johnson, C. D.; Katritzky, A. R.; Shapiro, S. A. *J. Am. Chem. Soc*. **1969**, *91*, 6654. Gillespie, R. J.; Peel, T. E.; Robinson, E. A. *J. Am. Chem. Soc.* **1971**, *93*, 5083.

(11) Land, E. J.; Porter, G.; Strachen, E. *Trans. Faraday Soc.* **1961**, *57*, 1885.

(12) Guha, S. N.; Moorthy, P. N.; Kishore, K.; Naik, D. B.; Rao, K. N. *Proc. Indian Acad. Sci. (Chem. Sci.)* **1987**, *99*, 261.

(13) Das, T. N. *J. Phys. Chem. A* **2001**, *105*, 9142.

(14) Buxton, G. V.; Stuart, C. R. *J. Chem. Soc., Faraday Trans.* **1995**, *91*, 279.

(15) Serjeant, E. P., Dempsey, B.; Eds. *Ionization Constants of Organic Acids in Solution*; IUPAC Chemical Data Series No. 23; Pergamon Press: Oxford, U.K., 1979.

(16) Jiang, P.-Y.; Katsumura, Y.; Nagaishi, R.; Domae, M.; Ishikawa, K.; Ishigure, K.; Yoshida, Y. *J. Chem. Soc., Faraday Trans.* **1992**, *88*, 1653.

(17) Domae, M.; Katsumura, Y.; Jiang, P. Y.; Nagaishi, R.; Ishigure, K.; Kozawa, T.; Yoshida, Y. *J. Chem. Soc., Faraday Trans*. **1996**, *92*, 2245.

(18) Sehested, K.; Rasmussen, O. L.; Fricke, H. *J. Phys. Chem*. **1968**, *72*, 626.

(19) Buxton, G. V.; Greenstock, C. L.; Helman, W. P.; Ross, A. B. *J. Phys. Chem. Ref. Data* **1988**, *17*, 513.

(20) Das, T. N. *Ind. Eng. Chem. Res*., in press.

(21) Ilan, Y. A.; Czapski, G.; Meisel, D. *Biochim. Biophys. Acta* **1976**, *430*, 209.

(22) Koppenol, W. H.; Butler, J. *Adv. Free Biol. Med.* **1985**, *1*, 91.

(23) Das, T. N.; Huie, R. E.; Neta, P. *J. Phys. Chem. A* **1999**, *103*, 3581. Lind, L.; Shen, X.; Eriksen, T. E.; Merenyi, G. *J. Am. Chem. Soc.* **1990**, *112*, 479.

(24) Mezyk, S. P.; Bartels, D. M. *J. Chem. Soc., Faraday Trans.* **1995**, *91*, 3127.

(25) Sweet, J. P.; Thomas, J. K. *J. Phys. Chem.* **1964**, *68*, 1363.

(26) Das, T. N.; Ghanty, T. K.; Pal H. *J. Phys. Chem. A* **2003**, *107*, 5998.

(27) Sehested, K.; Hart, E. J. *J. Phys. Chem.* **1975**, *79*, 1639.

(28) Hug, G. H. *Optical Spectra of Nonmetallic Inorganic Transient Species in Aqueous Solution*; NSRDS-NBS 69; National Bureau of Standards: Washington, DC, 1981; pp 54−55. Devonshire, R.; Weiss, J. J. *J. Phys. Chem.* **1968**, *72*, 3815.

(29) Schwarz, H. A.; Bielski, B. H. J. *J. Phys. Chem*. **1986**, *90*, 1445.

(30) Covington, A. K.; Matheson, R. A. *J. Solution Chem.* **1976**, *5*, 781.

(31) Elliot, A. J.; Geertsen, S.; Buxton, G. V. *J. Chem. Soc., Faraday Trans. 1* **1988**, *84*, 1101.

(32) Zehavi, D.; Rabani, J. *J. Phys. Chem.* **1972**, *76*, 312.

(33) Jayson, G. G.; Parsons, B. J.; Swallow, A. J. *J. Chem. Soc., Faraday Trans. 1* **1973**, *69*, 1597.

(34) Spinks, J. W. T.; Wood, R. J. *An Introduction to radiation Chemistry*, 3rd ed.; Wiley-Interscience, John Wiley and Sons: New York, 1990; pp 119−120.

(35) Swallow, A. J.; Inokuti, M. *Radiat. Phys. Chem.* **1988**, *32*, 185.

(36) Domae, M.; Katsumura, Y.; Ishigure, K.; Byakov, V. M. *Radiat. Phys. Chem.* **1996**, *48*, 487.

(37) Sulco Chemicals Ltd. *H_2SO_4 Tech. Bull*. **2002**, p 7. www.sulcochemicals.com.

(38) Land, E. J.; Ebert, M. *Trans. Faraday Soc.* **1967**, *63*, 1181.

(39) Dorfman, L. M.; Taub, I. A.; Buehler, R. E. *J. Chem. Phys.* **1962**, *36*, 3051.

(40) Ramanan, G. *J. Indian Chem. Soc*. **1977**, *53*, 957.

(41) Pan, X.-M.; von Sonntag, C. *Z. Naturforsch., B, Chem. Sci*. **1990**, *45B*, 1337.

(42) Alfassi, Z. B.; Huie, R. E.; Neta, P.; Shoute, L. C. T. *J. Phys. Chem.* **1990**, *94*, 8800.

(43) Hasegawa, K.; Neta, P. *J. Phys. Chem*. **1978**, *82*, 854.

(44) Willson, R. L. *Biochem. Soc. Trans.* **1973**, *1*, 929.

(45) Field, R. J.; Raghavan, N. V.; Brummer, J. G. *J. Phys. Chem*. **1982**, *86*, 2443.

(46) Adams, G. E.; Boag, J. W.; Currant, J.; Michael, B. D. In *Pulse Radiolysis*; Ebert, M., Keene, J. P., Swallow, A. J., Baxendale, J. H., Eds.; Academic Press: New York, 1965; p 131.

(47) Mvula, E.; Schuchmann, M. N.; von Sonntag, C. *J. Chem. Soc., Perkin Trans. 2* **2001**, 264.

(48) Roder, M.; Wojnarovits, L.; Földiak, G.; Emmi, S. S.; Beggiaro, G.; D'Angelantonio, M. *Radiat. Phys. Chem.* **1999**, *54*, 475.

(49) Braun, W.; Herron, J. T.; Kahaner, D. *Int. J. Chem. Kinet.* **1988**, *20*, 51.

(50) Ross, A. B.; Bielski, B. H. J.; Buxton, G. V.; Greenstock, C. L.; Helman, W. P.; Huie, R. E.; Grodkowski, J.; Neta, P.; Mallard, W. G. *NDRL-NIST Solution Kinetics database: Ver. 3*; National Institute of Standards and Technology: Gaithersburg, MD, 1994.

(51) Hermann R.; Mahalaxmi, G. R.; Jochum, T.; Naumov, S.; Brede, O. *J. Phys. Chem. A* **2002**, *106*, 2379.

(52) Das, T. N. *J. Phys. Chem. A* **2001**, *105*, 5954.

(53) Ye, M.; Madden, K. P.; Fessenden, R. W.; Schuler, R. H. *J. Phys. Chem.* **1986**, *90*, 5397.

(54) Tripathi, G. N. R.; Chipman, D. M. *J. Phys. Chem. A* **2002**, *106*, 8908.

(55) Badger, B.; Brocklehurst, B.; Russel, R. D. *Chem. Phys. Lett.* **1967**, *1*, 122.

(56) Badger, B.; Brocklehurst, B. *Trans. Faraday Soc.* **1969**, *65*, 2582.